Russian Geology and Geophysics © 2019, V.S. Sobolev IGM, Siberian Branch of the RAS
Vol. 60, No. 7, pp. 705–719, 2019 *DOI:10.15372/RGG2019033* *Geologiya i Geofizika*

Interaction of a Spreading Mantle Plume Head and the Ancient Lithosphere: Studying Mantle Xenoliths in Basalts and Lamprophyre Diatremes of Western Syria

E.V. Sharkov, O.A. Bogatikov

Institute of Geology of Ore Deposits, Petrography, Mineralogy, and Geochemistry of the Russian Academy of Sciences, Staromonetnyi per. 35, Moscow, 119017, Russia

Received 14 November 2017; received in revised form 12 February 2018; accepted 1 March 2018

Abstract—Our study of mantle xenoliths in the Cretaceous lamprophyre diatremes and late Cenozoic plateau basalts of western Syria has shown that the ancient lower crust that existed in the Cretaceous and was composed of garnet granulites and eclogite-like rocks was replaced by mantle peridotites in the late Cenozoic. We conclude that the heads of the local (secondary) plumes of the present-day Afro-Arabian thermochemical mantle plume responsible for the regional basaltic magmatism reached the basement of the ancient upper sialic crust, where they spread, leading to a displacement of the mafic lower crust.

Keywords: thermochemical mantle plumes, large igneous provinces, mantle xenoliths, lower crust, mantle fluids, Syria

INTRODUCTION

Most researchers currently share the assumption that present-day tectonomagmatic activity of the Earth is associated with ascent of thermochemical mantle plumes originating at the boundary between the outer iron core of the Earth and its silicate mantle (Maruyama, 1994; Artyushkov, 1995; Dobretsov et al., 2001; etc.), which has been confirmed by recent seismic tomography data (French and Romanowicz, 2015). However, it still remains unclear what the exact composition of mantle plumes is; what happens, when they penetrated in the ancient continental lithosphere; and how this process affects on deep structure in conerete regions.

Identification of the material composition of thermochemical plumes is complicated by the fact that, as opposed to the silicate upper mantle, the lower and especially lowermost mantle is formed by juvenile ultramafic association composed primarily of oxides (bridgmanite, ferropericlase, CaSi-perovskite, and free silica); moreover, the overall composition of the lower mantle deviates from the pyrolitic model due to increased silica content and the presence of free silica (Kaminsky, 2017). Thus, as the lower mantle matter rises towards the surface, its mineral composition is expected to transform significantly turning it into the silicate mantle rocks typical for moderate depths.

It is believed that thermochemical mantle plumes are generated within the 200 km-thick D″ layer, which developed along the contact area of the mantle with the outer liquid iron core. Here, ferriferous fluid/melt with 5–10% content of light elements (C, N, O, and Si) infiltrates in the lowermost mantle from the outer core, and partial melting of the carbon-bearing matter of the lower mantle forms a carbonatite melt that is further enriched with P, F, Cl, and other volatile elements at the core-mantle boundary (Kaminsky, 2017). This seems to be the process leading to enrichment of thermochemical plumes with fluid components. Since the crystallization products of these fluids/melts ("black" series xenoliths in basalts, see below) are enriched with Ti, Ba, alkalis, rare earths, and other incompatible elements, these components also appear to come from the liquid core together with the fluids (Sharkov and Bogatikov, 2015b).

The mantle plume matter is characterized by increased buoyancy due to the presence of the fluids and, according to the experimental data, may rise to moderate depths (Kirdyashkin and Kirdyashkin, 2016). As a result, the extension of mantle plume heads in the lithospheric mantle becomes the primary driving force of tectonic processes, while adiabatic melting of the mantle matter leads to the large-scale intraplate basaltic magmatism manifested as large igneous provinces (LIP) and hot spots (Yarmolyuk and Kovalenko, 2003; Bogatikov et al., 2010; Ernst, 2014). The presence of the core matter in these mantle plumes is indicated by Os isotope studies of LIP basalts (Walker et al., 1997; Brandon et al., 1999; Puchtel et al., 1999).

It follows from the available data on the structure of Phanerozoic LIPs, which typically consist of several subprovinces (for instance, the Siberian LIP (Zolotukhin et al., 1986)), that the spreading of the mantle plume head was ac-

✉ Corresponding author.
E-mail adress: sharkov@igem.ru (E.V. Sharkov)

companied by the occurrence of secondary plumes, or protuberances distributed over its surface. The rising of those protuberances was the most likely caused by local accumulations of volatile components, which ensured additional buoyancy of the mantle plume matter (Dobretsov et al., 2006). The plumes reached moderate depths, and adiabatic melting of their heads led to formation of magmatic systems.

According to the geological data and geochemical properties of magmatism in LIPs, it was not until the middle Paleoproterozoic (about 2.35 Ga) that thermochemical mantle plumes occurred on a mass scale change the early Precambrian thermal plumes formed by depleted ultramafites and thereby becoming the key phenomenon to define the fundamental features of the Earth's geodynamic development (Sharkov and Bogatikov, 2010). However, it was already mentioned that it still remains unclear what the exact composition of thermochemical plumes is, what depths the plume heads can reach, and what occurs, when the plumes penetrate the lithosphere, and their heads extend within it. The deep-seated xenoliths transported to the surface by alkaline Fe–Ti basalts and basanites represent one of the few sources of petrological information on these processes that are available for direct observation.

As opposed to fragments of lithospheric mantle in kimberlite and lamproite pipes (diatremes) where various garnet ultramafites and eclogites, including the diamond-bearing ones, develop (Sobolev, 1977; Dawson, 1980; Laz'ko, 1988; etc.), mantle xenolith populations in intraplate (i.e. associated with mantle plume ascent) moderately-alkaline Fe–Ti basalts and basanites around the world, in both continental and oceanic environments, show a remarkable uniformity (Ionov, 1988; Pearson et al., 2003). Mantle xenoliths are mostly represented by the two major groups: (1) more common spinel peridotites (occasionally with a small presence of garnet) of the "green", or Cr-diopside series, and the rarer (2) formations of the "black", or Al–Ti-augite series, which form veins in the "green" series rocks (Fig. 1).

The noteworthy uniformity of mantle xenoliths around the world as well as the similarity of the host intraplate moderately alkaline Fe–Ti basalts of OIB-type (oceanic island basalts) regardless of the specific geological setting, may only be achieved due to the uniform composition of thermochemical mantle plumes, which are responsible for their formation and are inherently of the same origin. Therefore, we assume that mantle xenoliths are the fragments of the upper margins of mantle plume heads, cooled in the contact with the relatively cold ancient lithosphere. They are transported by the newly formed basalts arrived from the underlying adiabatic melting zone and in our opinion, represent the samples of the plume matter itself (Sharkov and Bogatikov, 2015a; Sharkov et al., 2017). Spinel peridotites seem to represent the primary matter of mantle plume heads which was not subjected to the adiabatic melting occurring in the areas within the heads located the farthest from the contact areas. Thus, they most likely represent the lower mantle rocks, transformed under moderate depth conditions. The presence of orthopyroxene in these lherzolites indicates the increased

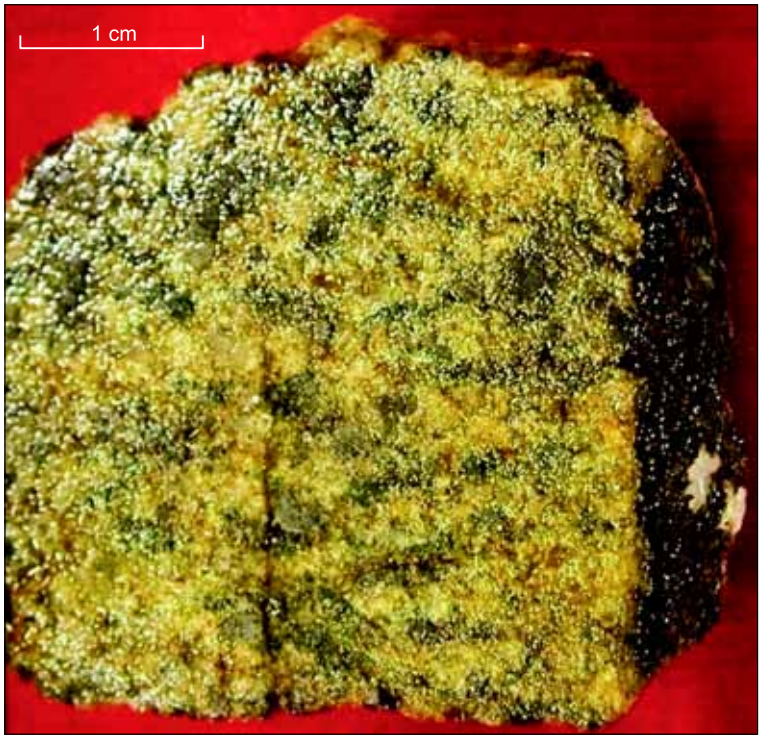

Fig. 1. "Black" series vein (right) in the green spinel lherzolite. Photo by H. Downes, personal presentation.

free silica content in the protolith, which is typical for the lower mantle rocks (see above).

Spinel lherzolites seem to include traces of high-density fluids of the Earth's core preserved in the form of films enriched with incompatible elements located between peridotite grains, which are found in mantle xenoliths in basalts from both continental rifts and oceanic islands (Grachev and Komarov, 1994). It will be shown below that these fluids were most likely released as a result of decompression degassing while still in the mantle setting. They participated in adiabatic melting of the plume head, while their excessive amounts were involved in metasomatic processes that led to local incongruent ("secondary") melting of peridotites in the cooled upper margin of the plume head with formation of parent fluids/melts for the "black" series rocks (see below).

The cases, in which ascent of mantle plumes, accompanied by basaltic magmatism, is preceded by lamprophyre or kimberlite pipes (diatremes) with xenoliths of the ancient lithospheric rocks, i.e., when the information on the deep structure of the region before and after the plume uplift is available, are of special interest in terms of understanding the relationship between the lithosphere and mantle plumes. Western Syria (Fig. 2) is the such region. It located within the late Cenozoic Afro-Arabian LIP (Ernst, 2014) where closely placed areas of location of lower crustal xenoliths in Middle Cretaceous lamprophyre diatremes (Sharkov et al., 1992) and mantle xenoliths in Cenozoic moderately alkaline basalts (Sharkov et al., 1996, 2017). Thus, the goal of the present paper is to discuss the problems of composition of the thermochemical mantle plume head and its interaction with the ancient lithosphere. For shortening the text, the data used were, with a few exceptions, taken from the chemical and microprobe studies published earlier works and referenced in the text.

MANTLE XENOLITHS IN PLATEAU BASALTS OF WESTERN SYRIA

The territory of Syria is an ancient platform with Precambrian basement formed by Archean and Paleoproterozoic gneisses and migmatites, but mostly by Neoproterozoic volcanosedimentary rocks developed in course of the Pan-African orogeny under conditions of continental rifting and island arcs (Stern et al., 1991, 2016). While the region was at its platform evolution stage in the Paleozoic and Mesozoic, it became an area of intense intraplate magmatism starting from the middle Miocene, with the last magmatic activity outbursts taking place in the written history era (Ponikarov et al., 1969). So, while Cretaceous diatremes include xenoliths of the ancient lower crust, the mantle xenoliths in late Cenozoic basalts reflect the present-day material composition of the mantle in the region.

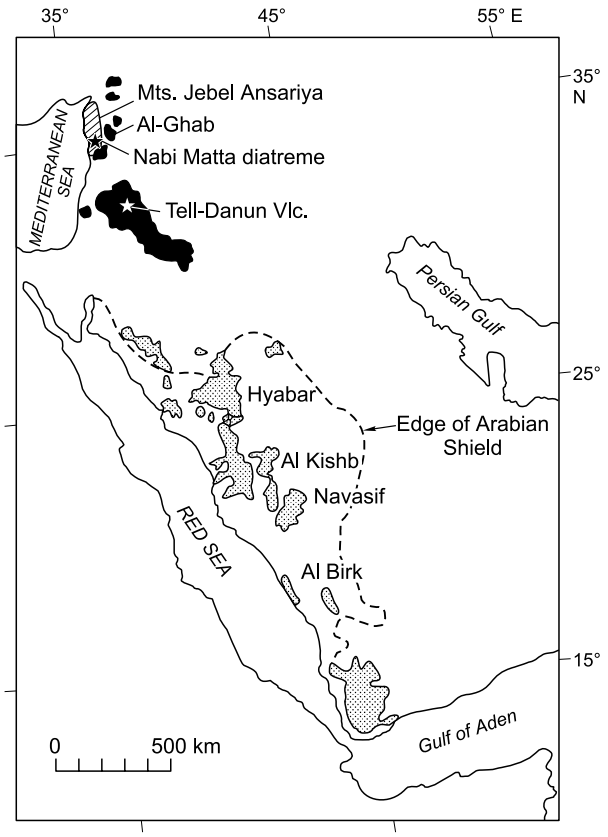

Fig. 2. Late Cenozoic basaltic plateaus of Arabia. Main basaltic plateaus of Arabia are shown in gray; the studied basaltic plateaus are shown in black.

Mantle xenoliths in basalts of western Syria

Research method. Contents of petrogenic and rare elements in rocks were determined via X-ray fluorescence using a PW 2400 PHILIPS X-RAY SPECTROMETER. Contents of rare and rare earth elements in some samples were determined by ICP-MS using the VG INSTRUMENTS PLASMA QUARD PQ2+TURBO quadrupole mass spectrometer. All measurements were performed in the Laboratory of Mineral Analysis of IGEM RAS.

Syria is a classic example of late Cenozoic plateau basalt development associated with the Afro-Arabian mantle plume uplift, whose roots, according to the seismic tomography data, are located at the core-mantle boundary (Hansen et al., 2012). Thus, what we are dealing with is the manifestation of a thermochemical mantle plume in a general sense and therefore the conclusions drawn seem to be applicable to the most similar cases. Geological, petrological, and geochronological data (Sharkov and Lebedev, 2017), as well as seismic tomography data (Schaeffer and Lebedev, 2013; Faccenna et al., 2013), indicate that the mantle plume matter gradually flows in the lithosphere at depths of 50–100 km in the northern rhumbs forming what might be called an arm stretching from the Afar hot spot to the north throughout the

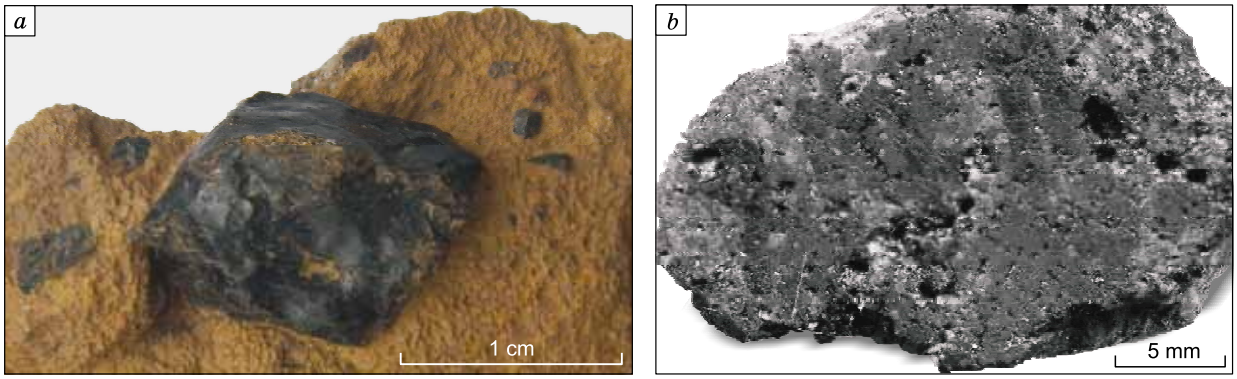

Fig. 3. Melted kaersutite megacryst in the basaltic pyroclastic matter (*a*), and gas cavities in the "black" series xenolith (*b*). Tell-Danun Volcano, southern Syria (E.V. Sharkov's collection).

whole western part of the Arabian Peninsula up to the Caucasus. This arm along its whole length is traced at the surface by large late Cenozoic basaltic plateaus that appear to develop above the protuberances (secondary plumes) at the surface of the plume.

Mantle xenoliths in basalts were studied in the Quaternary volcanoes of Syria: Tell-Danun in southern Syria, Harrat Ash Shamah volcanic field, and Tel Ghazal pyroclastic cone in the Al-Ghab plateau in northwestern Syria (Fig. 2), where xenoliths of both "green" and "black" series were observed (Sharkov et al., 1996, 2017).

Like in most cases, xenoliths of the "green" series are represented by light green spinel peridotites with cataclastic or less common protogranular structure; they are characterized by the presence of Cr-diopside and very stable composition of high-Mg olivine and pyroxene (mg# 88-92). Prevalent components of peridotite compositions vary from spinel lherzolites to depleted spinel harzburgites and even spinel dunites; occasionally, green spinel pyroxenites (predominantly websterites) are encountered. The latter form veins in the peridotite matrix and are often characterized by the presence of thin grossular-almandine-pyrope garnet rims around spinel grains (Sharkov et al., 1996). Since some xenoliths of the "green" series include minerals, such as kaersutite, phlogopite, apatite, carbonate, etc., it means that they are locally and to various extent subjected to mantle metasomatism (Sharkov et al., 1996).

Al–Ti-augites and aqueous phases, such as hornblende (kaersutite-pargasite group) and phlogopite, as well as rhonite (Ryabchikov et al., 2010), are significant components of "black" series xenoliths, as opposed to those of the "green" series; olivine and pyroxene here are more ferrous (mg# < 85). "Black" series formations are represented by wehrlites, clinopyroxenites, amphibolic and phlogopite clinopyroxenites, kaersutite hornblendites, etc. Fragments of coarse-grained rock types of the same series are represented by Al–Ti-augite, kaersutite, olivine, ilmenite, sanidine, and other megacrysts with lengths of 5–10 cm. Megacrysts, especially kaersutite, often include multiple gas cavities, which implies high-density fluids/melts as their sources of origin, and they often have melted edges, as opposed to lherzolites (Fig. 3).

The origin of "black" series rocks remains a matter of discussion. A. Irving (1980) considered them as the result of crystallization of basanite magma that infiltrated the mantle substrate along the cracks and reacted with the host rocks generating water-bearing minerals. This model is difficult to accept, since the "black" series differs in their mineral composition from basalts and basanites, especially in terms of prevalence of water-bearing minerals. Contrary to A. Irving, Wilshire et al. (1980) assumed that formation of veins was associated with infiltration of the iron-rich aqueous fluid that crystallized in the form of kaersutite into lherzolites. According to the authors, the fluid reacted with host lherzolites, which led to significant changes in mineral and rock compositions. V.I. Kovalenko et al. (1986) also came to conclusion that fluids were involved in mantle mineral formation, as a result of their studies of mantle xenoliths from the alkaline-basaltic volcano Shavaryn Tsaram in Mongolia. They showed that compositions of mafic minerals and captive minerals in microinclusions were practically the same, which had to do with high-density fluid/melt being their source of origin. In other words, the important role of fluid components in petrogenetic processes in mantle plume heads is currently beyond any doubt.

It is further confirmed by geochemical peculiarities of xenoliths and megacrysts, as well as moderately alkaline Fe–Ti host basalts, in Tell-Danun Volcano studied by the authors of the present paper (Table 1). It can be seen from Fig. 4 that depleted spinel peridotites are characterized by low contents of incompatible elements and differ significantly from "black" series formations (in this case, kaersutite megacrysts), which, in turn, are close to geochemically enriched alkaline-basaltic lavas in terms of composition. Hence, we infer that the specific geochemistry of intraplate basalts in context of depleted peridotite substrate of the mantle plume could only be provided by the presence of fluid components enriched with Fe, Ti, alkalis, light rare earth elements, Ba, Nb, Ta, and other incompatible elements in the adiabatic melting area (Sharkov et al., 2017).

Table 1. Compositions of mantle xenoliths and host basalts, Tell-Danun Volcano, southern Syria (Sharkov et al., 2017)

Component	Sample No.										
	149/16	814-1	819-26	20/12-1	217/2-2	814/12	814-4	814-10	819-17	814/5	814/9
	1	2	3	4	5	6	7	8	9	10	11
SiO_2	47.32	44.73	44.90	44.28	43.67	39.81	38.93	40.55	41.58	41.28	44.46
TiO_2	2.43	2.59	2.68	4.43	5.04	5.67	0.07	0.24	0.09	0.07	0.17
Al_2O_3	14.91	14.97	14.00	13.40	13.33	14.03	1.09	1.70	2.44	2.04	3.46
Fe_2O_3*	13.06	14.41	14.29	13.40	13.74	11.21	8.84	13.71	11.71	9.07	7.70
MnO	0.15	0.20	0.20	0.11	0.06	0.10	0.14	0.22	0.18	0.14	0.13
MgO	9.20	8.69	8.72	10.96	9.17	13.12	45.22	40.89	40.35	44.04	38.62
CaO	9.57	8.52	8.61	10.63	9.41	10.83	0.97	1.67	1.91	1.68	3.58
Na_2O	2.75	3.76	3.49	2.40	2.86	2.60	0.12	0.19	0.34	0.16	0.32
K_2O	0.82	1.17	1.58	0.88	1.46	1.59	0.03	0.05	0.11	0.06	0.10
P_2O_5	0.31	0.63	0.71	0.16	0.12	0.03	0.02	0.03	0.03	<0.02	<0.02
LOI	N/A	<0.10	<0.10	N/A	N/A	0.70	3.81	<0.10	0.22	0.28	0.52
Total	100.5	99.67	99.18	100.65	98.86	99.69	99.24	99.25	98.96	98.82	99.08
Li	N/A	7.7	15	N/A	N/A	5.5	1.9	6.6	11	2.7	2.4
Sc	24.2	22	16	26.8	24.2	32	7.7	8.0	11	6.8	16
V	N/A	185	185	N/A	N/A	524	34	45	46	32	89
Cr	392	187	248	52.3	18	16	1802	2590	2094	986	1216
Co	64.9	51	52	78.7	86.7	65	118	112	111	108	88
Ni	430	164	204	267	518	188	2419	2011	2075	2227	1953
Cu	N/A	58	76	N/A	N/A	52	7.4	10	18	5.9	60
Rb	25.3	12	18	10.5	N/A	4.9	0.67	1.2	2.3	0.70	0.64
Sr	622	816	776	575	N/A	473	20	26	38	8.5	11
Y	N/A	23	22	N/A	N/A	14	0.79	2.2	2.0	1.5	2.9
Zr	143	279	272	98	93	46	7.2	12	12	3.1	6.4
Nb	N/A	39	49	N/A	N/A	12	1.5	1.2	2.2	0.16	0.35
Ba	155	195	413	119	191	130	16	64	30	30	7.0
La	15.6	31	35	5.56	5.77	3.5	1.0	0.92	1.7	0.44	0.67
Ce	36.3	65	73	16.7	19.3	12	2.2	2.7	4.3	0.65	1.3
Pr	N/A	8.0	9.0	N/A	N/A	2.2	0.27	0.43	0.60	0.12	0.21
Nd	16.6	32	35	13.8	16.1	13	0.98	2.2	2.6	0.56	1.1
Sm	4.5	6.9	7.6	4.62	5.13	4.0	0.22	0.63	0.54	0.15	0.37
Eu	1.53	2.3	2.8	1.66	1.64	1.5	0.09	0.26	0.22	0.072	0.13
Gd	N/A	6.2	7.0	N/A	N/A	4.3	0.19	0.56	0.52	0.17	0.49
Tb	0.78	1.0	1.0	0.69	0.65	0.67	0.033	0.10	0.079	0.027	0.080
Dy	N/A	5.2	5.2	N/A	N/A	3.6	0.18	0.52	0.41	0.27	0.57
Ho	N/A	1.0	0.94	N/A	N/A	0.63	0.031	0.088	0.076	0.058	0.14
Er	N/A	2.4	2.2	N/A	N/A	1.4	0.074	0.20	0.22	0.17	0.40
Tm	N/A	0.34	0.32	N/A	N/A	0.18	0.010	0.029	0.026	0.026	0.055
Yb	1.598	2.0	1.8	1.22	0.672	0.83	0.080	0.19	0.20	0.16	0.37
Lu	0.248	0.28	0.25	0.181	0.073	0.11	0.009	0.020	0.032	0.022	0.049
Hf	3.72	5.6	5.6	2.24	2.72	1.5	0.06	0.14	0.23	–	0.015
Ta	1.86	2.2	2.7	0.88	1.31	0.96	0.21	0.007	0.18	0.048	0.085
Pb	N/A	3.8	6.4	N/A	N/A	1.7	1.4	2.0	0.88	2.2	0.38
Th	1.19	2.7	3.0	2.16	1.9	N/A	0.12	0.091	0.13	–	–
U	2.07	0.89	0.96	N/A	N/A	0.020	0.047	0.071	0.046	0.017	0.052

Note. Contents of main components in are measured in wt.%, rare and rare earth elements in ppm, N/A, contents were not identified; bdl, contents below detection limit. Rocks: 1–3, host basalts; 4–6, kaersutite; 7, Sp harzburgite; 8–11, Sp lherzolite. E.V. Sharkov's collection (Sharkov et al., 2017). Measurements were performed at the Common Use Center IGEM-Analitika.

*Total iron in the form Fe_2O_3.

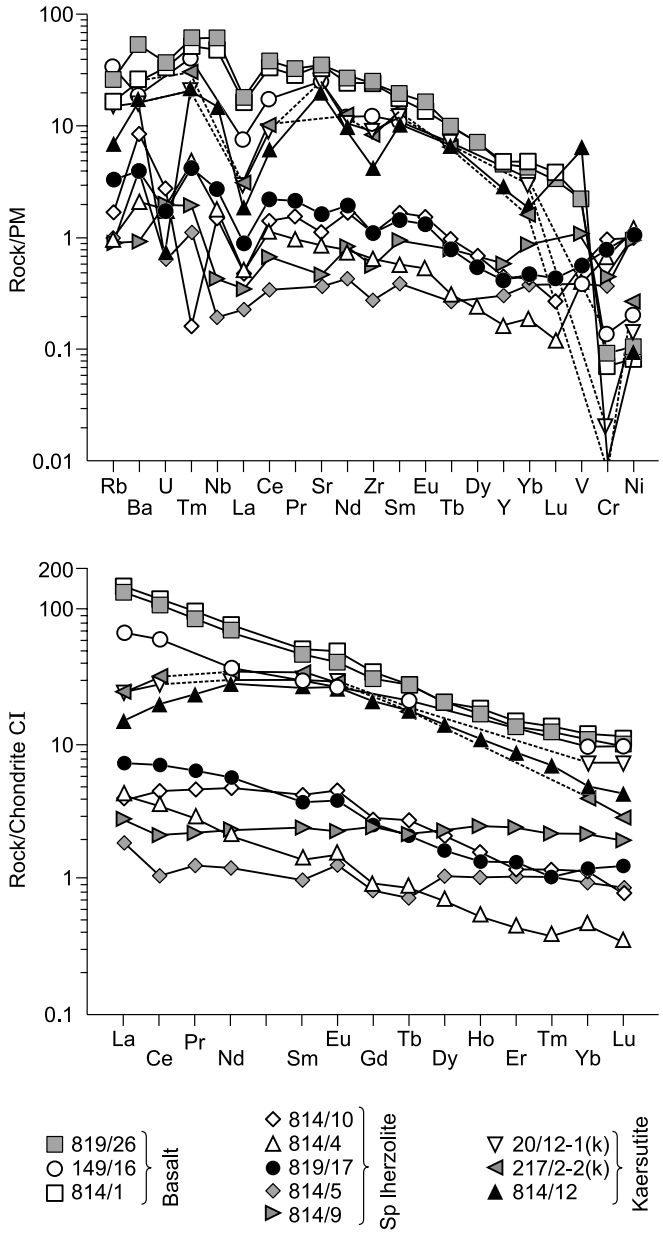

Fig. 4. Element contents in mantle xenoliths and host basalts normalized by primitive mantle (PM) and rare earth element contents normalized by chondrite C1. Tell-Danun Volcano, southern Syria.

Thus, the composition of xenoliths indicates that the upper cooled margin of the plume head was formed by the two main types of matter: (1) the matrix consisting of depleted ultramafic "green" series rock and (2) veins of "black" series rocks that crystallized from the high-density fluid/melt.

Mantle fluids

The presence of two mantle metasomatism agents was revealed in mantle xenoliths in Pliocene–Quaternary plateau basalts of the Al-Ghab plateau (Ma et al., 2015), as well as in intraplate late Cenozoic basalts in Europe (Downes, 2001). The earlier of the two, the carbonatite-type agent, which infiltrated the peridotite matrix, was a highly mobile low-silicate CO_2-rich fluid/melt enriched with light rare earth elements, Na, Th, U, and Ba.

The second, i.e. silicate, type of fluid/melt, which manifested itself before the eruption, was characterized by influx of Ti, Fe, P, K, Nb, Ta, Cs, and other incompatible elements, as well as water. It is associated with the occurrence of lenticules formed by fine-grained aggregate of olivine, Al–Ti-augite, amphibole (kaersutite), Ti-phlogopite, sanidine, andesine, ilmenite, and other "black" series minerals, as well as volcanic glass with trachyte composition in peridotites (Fig. 5). These lenticules are considered as solidified melt-pockets that occurred as a result of incongruent ("secondary") peridotite melting (Ryabchikov et al., 2010; Ma et al., 2015), and which were formed in the peridotites within the cooled upper margin of the spreading mantle plume head (Sharkov and Bogatikov, 2015a). When ruptures occur in the rocks of the latter rim, the newly formed secondary melt was pressured into them with generation of vein-like shapes.

Thus, the presence of at least two mantle metasomatism agents has been established, which seem to have previously existed in the form of high-density phases in the intergranular space of the peridotite matrix of the plume; they were released in course of decompression and were involved in adiabatic melting processes, thereby ensuring the geochemical peculiarities of basalts.

Since mantle xenoliths are mostly encountered in pyroclastic and cinder cones and rarely found in lavas, excesses of the fluids that did not dissolve in the newly formed basaltic melt, were accumulated above the adiabatic melting zone under the cooled margin of the plume head and seemingly formed bubble-like shapes. Occasionally, they either burst to the surface in the form of pyroclastic matter or were pres-

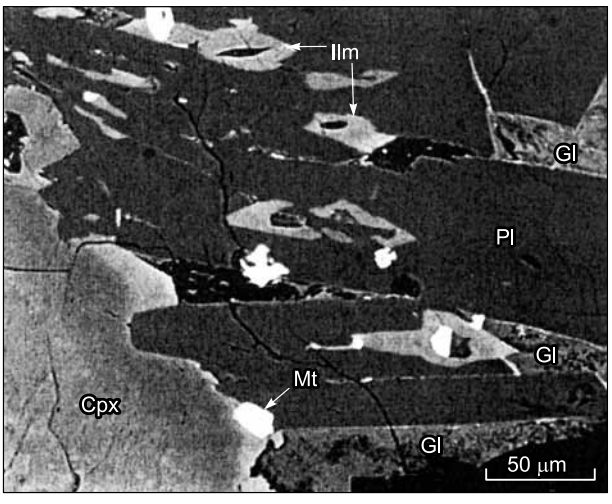

Fig. 5. Devitrificated melt-pocket in the spinel lherzolite. Plagioclase (Pl), magnetite (Mt), ilmenite (Ilm), and devitrified glass with trachyte composition (Gl); on the left—spongy primary clinopyroxene (Cpx). Backscatter electron (BSE) image (Ryabchikov et al., 2010).

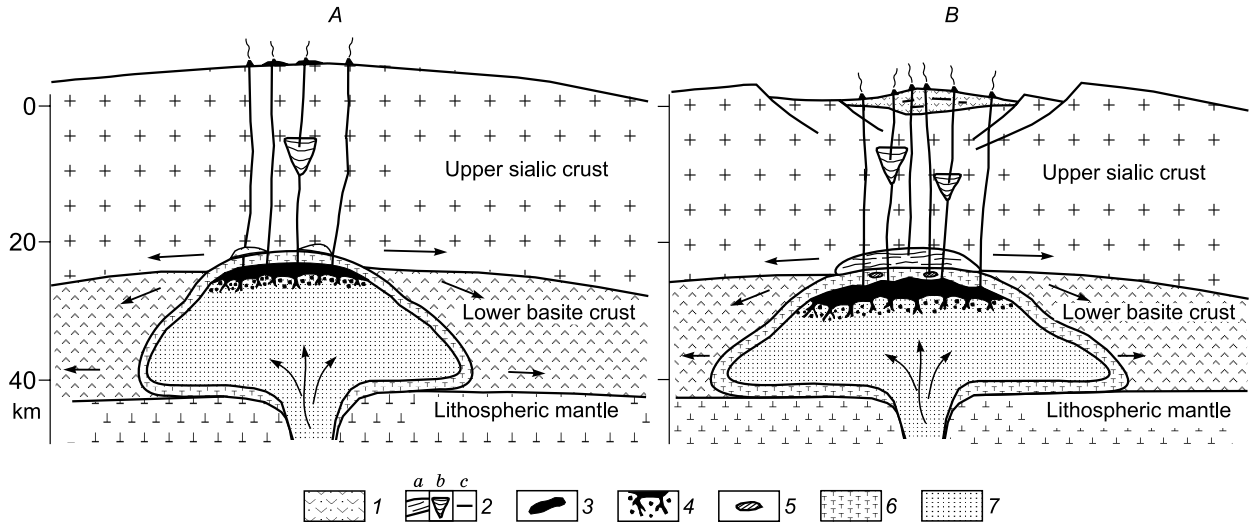

Fig. 6. Structure chart of magmatic systems of large igneous provinces: *A*, initial stage; *B*, mature stage. *1*, volcanosedimentary rocks, *2*, intermediate magmatic chamber: *a*, at the boundary between the plume head and the crust (underplating), *b*, layered mafite–ultramafite intrusions, *c*, shallow sills; *3*, basaltic melt; *4*, adiabatic melting zones; *5*, restites; *6*, cooled margin of the plume head; *7,* fresh plume material arrived to the mantle plume head.

sured to the surface in the form of cinder, while transporting large amounts of xenoliths. Fluids infiltrated the peridotites of the cooled rim between these eruptions, which eventually led to the occurrence of incongruent (secondary) melting foci. These melting processes are considered in detail for the case of xenoliths from Syria in (Ryabchikov et al., 2010; Ma et al., 2015), and are therefore left beyond the scope of the present paper.

The use of various geothermal barometers (Brey and Köhler, 1990; Witt-Eickschen and Seck, 1991; Taylor, 1998; Putirka, 2008) showed that primary peridotites of the "green" series were formed at depths of 24–42 km (0.8–1.4 GPa) at 896–980 °C and locally up to 1030 °C (Ryabchikov et al., 2010; Ma et al., 2015). Melt-pocket minerals (of the "black" series) were formed at temperatures of 826–981 °C at depths of 21–27 km (0.7–0.9 GPa); in other words, the plume head here reached the depth of 21 km. It is approximately the depth of the basement of the sialic crust of the Arabian plate (Stern et al., 2016), which agrees well with rarity of lower crustal xenolith discoveries in the studied populations.

The proposed development pattern of magmatic systems in LIPs associated with mantle plume heads is presented in Fig 6. Since mantle xenoliths are only observed in moderately alkaline Fe–Ti basalts at initial evolutionary stages of these magmatic systems, we assume that these basalts were the first subjected to adiabatic melting of the mantle plume head. As magmatic systems developed, intermediate chamber (large layered mafite-ultramafite intrusions) arose, where accumulation of melts, their crystallization differentiation, mixing of magmas and their contamination with host rock material occurred, which is why lavas rising towards the surface could be significantly different from the initial ones (Sharkov and Bogatikov, 2015a). The largest chambers developed along the boundary between the plume head and the overlaying lithosphere, which led to underplating as interpreted by R. Rudnick (1960) (Fig. 6*b*). Fragments of rocks from the underplating zone are encountered in lavas in the form of autoliths gabbro and ferrogabbro.

It follows from the data presented that:

1. The "green" and "black" series xenoliths under study are most likely the fragments of the cooled thick upper margin of the plume head located at depths from 21 to 27 km; its temperature varied from 826 to 981 °C (locally up to 1030 °C). These xenoliths represent the two main types of mantle plume matter (peridotite matrix and fluid components) involved in magma formation.

2. The peridotite matrix of the cooled upper margin of the plume head is formed by depleted ultramafic material of the deep-seated spinel facies that was not have time to homogenize as it was rising from the depth of 42 km to 21 km.

3. Mantle fluids involved in generation of basaltic magmas and mantle metasomatism in mantle plume heads were initially present in the plume matter, and, in our opinion, those could be the fluids arrived from the liquid core during the thermochemical plume formation. According to the data obtained on metasomatism processes, incongruent melting, and composition of "black" series rocks, Fe, Ti, Si, Na, K, P, Ba, Nb, Ta, light rare earth elements, etc., as well as water and CO_2 were significant components of these fluids.

4. Two independent types of the melts associated with mantle plumes have been determined: (a) vastly prevalent products of adiabatic melting of mantle plume heads (basalts); and (b) products of incongruent peridotite melting in the cooled outer margins of mantle plumes heads in presence of hot fluids transported from the underlying adiabatic

melting zone ("black" series rocks, including megacrysts and volcanic glass with trachyte composition) as a subordinate phenomenon.

LOWER CRUSTAL XENOLITHS IN CRETACEOUS LAMPROPHYRE DIATREMES OF WESTERN SYRIA

These diatremes were studied by the authors during joint Soviet-Syrian research efforts in the 1980s in western Syria in cooperation with Syrian geologists S. Hanna, H. Bassam, S. Ali, and E. Jermakani, and with a team of researchers from Novosibirsk led by N.V. Sobolev (Sobolev et al., 1990). Diatremes are usually represented by oval craters in Jurassic and Lower Cretaceous limestones of 500–1500 m in diameter and with depths of 400–500 m (Fig. 7) or less commonly by pyroclastic lenses (Fig. 8). Pyroclastic rocks with lower crustal xenoliths (spinel gabbro-norites, garnet gabbro, garnet granulites, eclogite-like rocks, as well as garnet, kaersutite, high-Al augite and other megacrysts) and small basalt flows are observed at their bottoms. A chain of such diatremes (Rband, Burgal, Kadmus, etc.) can be traced from the Kardaha region to the south, up to the city of Haifa (Mount Carmel) in Israel. Based on the geological and isotopic (K–Ar) data, these diatremes were formed between 123 and 110 Ma (Esperanca and Garfunkel, 1986; Mittlefehld, 1986; Sharkov et al., 1988).

The largest diatreme of the Mount Nabi Matta is located in the southern part of the Jebel Ansariya Ridge about 70 km to the south from the city of Latakia. It is a pyroclastic lens with lamprophyre composition (Table 2) with the area of ~40 km^2 and thickness up to 100–150 m (Fig. 8). Pyroclastic matter penetrates Albian–Aptian limestones with the Cretaceous basaltic flow and is overlaid by Cenomanian limestones and then by moderately-alkaline Pliocene Fe–Ti basalts of the adjacent minor volcano Jebel Seida, which includes xenoliths of spinel lherzolites. Thus, it is possible to observe deep-seated xenoliths of various ages and compositions here within a small area.

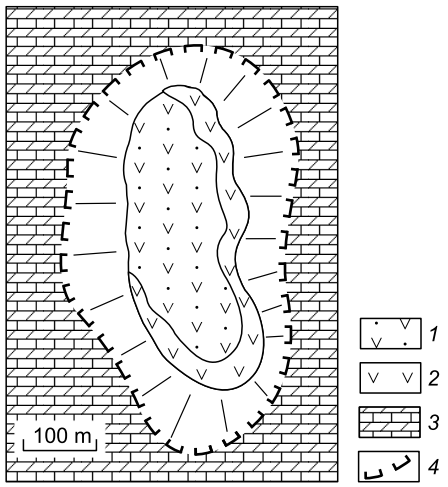

Fig. 7. Geological map of the Rband diatreme. *1*, weathering crust along the pyroclastic matter partially overlapped by modern sediments; *2*, lamprophyre pyroclastic matter with volcanic basaltic bombs, lower crustal xenoliths, and megacrysts; *3*, Jurassic limestones and dolomites; *4*, diatreme edges.

Deep-seated xenolith populations in the Nabi Matta diatreme

Xenolith populations in the Nabi Matta diatreme are represented by the following three groups: (1) garnet granulites and eclogite-like rocks; (2) garnet megacrysts and splices of garnet and high-Al augite; and (3) pegmatoid garnet-clinopyroxene-hornblende rocks (Sharkov et al., 1992; Sharkov and Bogatikov, 2015c). All the xenoliths usually have irregular oval or rounded (nodular) shapes and often melted edges.

Eclogite-granulite rocks that are typical for the continental lower crust are the prevalent group of xenoliths accounting for about 70% of the whole population. They sometimes preserve relicts of cumulative structures. Hence, it would be more correct to call them garnet ferrogabbro and garnet ferroclinopyroxenites, and that is exactly how these xenoliths

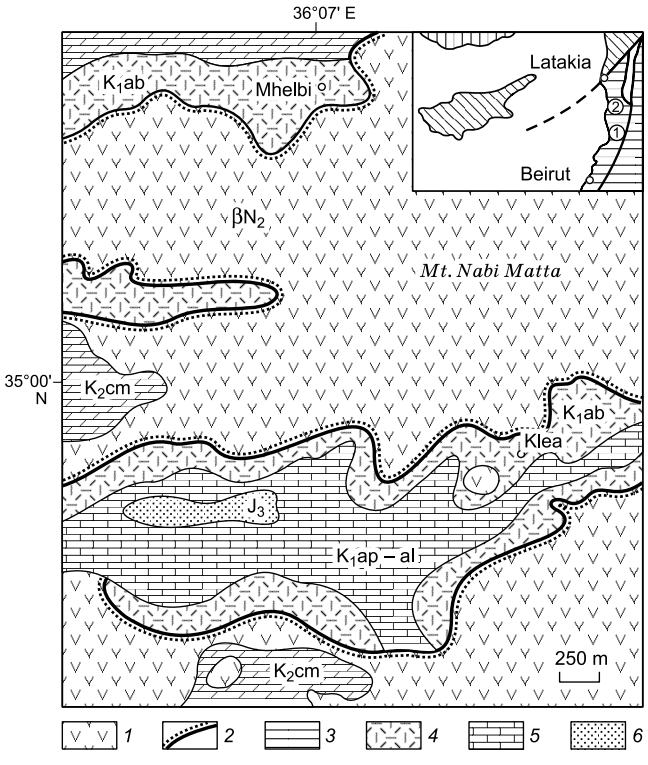

Fig. 8. Geological structure chart of the Nabi Matta lamprophyre diatreme. *1*, Neogene basalts; *2*, Cretaceous basaltic flow; *3*, Cenomanian limestones; *4*, pyroclastic matter with lamprophyre composition; *5*, Aptian–Albian limestones; *6*, Jurassic limestones. The insert: *1*, Nabi Matta diatreme location; *2*, lamprophyre diatremes in the Kardaha region.

Table 2. Chemical compositions of the rocks of the Nabi Matta diatreme and lower crustal xenoliths based (Sharkov et al., 1992)

Component	138-1	122	124-4	72-1	72-2	125-7	138-8	164-4	125-6	138-9
	1	2	3	4	5	6	7	8	9	10
SiO_2	28.70	35.30	45.62	43.00	44.75	46.00	40.46	50.16	47.22	40.80
TiO_2	1.78	0.84	1.16	2.26	2.02	0.72	4.53	2.21	3.04	0.55
Al_2O_3	7.20	9.61	17.97	13.30	12.39	11.08	14.28	14.08	17.59	22.20
Cr_2O_3	0.02	0.06	0.04	–	0.06	0.30	0.08	0.03	–	0.01
Fe_2O_3	5.02	5.00	5.16	6.44	5.06	3.60	5.79	5.35	2.90	2.05
FeO	3.13	4.23	7.58	5.06	8.65	6.00	12.24	6.72	6.38	10.00
MnO	0.11	0.22	0.35	0.16	0.16	0.37	0.19	0.19	0.15	0.31
MgO	12.71	17.45	6.20	11.77	9.46	13.27	10.54	7.05	7.86	17.14
CaO	17.95	9.44	9.96	10.36	9.36	14.64	8.01	5.93	9.84	4.80
Na_2O	0.36	0.70	2.28	2.80	2.24	1.10	0.96	2.14	2.25	0.10
K_2O	0.90	0.96	0.76	1.03	1.14	0.70	0.94	2.50	1.10	0.59
P_2O_5	0.38	0.50	0.41	0.62	0.55	0.02	0.02	0.62	0.01	n.i.
V_2O_5	0.02	0.02	0.04	–	–	0.05	0.07	0.05	–	0.03
NiO	0.03	0.02	0.01	–	0.03	0.03	0.04	0.01	–	0.01
CoO	0.01	0.02	0.01	–	0.01	0.01	0.01	0.01	–	0.01
SO_3	–	0.04	0.01	0.01	–	0.07	0.11	0.11	0.18	0.44
CO_2	12.77	6.43	0.00	0.79	0.00	0.06	–	–	0.32	–
$H_2O^{\pm}$	9.05	9.01	3.19	3.12	3.53	2.73	1.33	2.73	0.85	0.84
Total	100.14	99.85	100.75	100.72	99.55	100.75	99.60	99.88	99.69	99.88

Note. 1–2, lamprophyre pyroclastic matter; the total in the sample 1 also includes the following (wt.%): BaO = 0.16 and SrO = 0.039; 3, basaltic bomb in the pyroclastics; 4–5, overlapping Neogene basalts; 6–10, xenoliths: 6–7, eclogite-like rocks; the total in samples 6 and 7 also includes the following (wt.%): Rb_2O = 0.0019 and 0.0016, SrO = 0.0020 and 0.0109; BaO = 0.0071 and 0.0016; 8–9, garnet granulites; 10, garnet megacryst, n.i., not identified.

are referred to in the similar diatreme of the Mount Carmel (Esperanca and Garfunkel, 1986; Mittlefehld, 1986). However, in addition to the relicts of cumulative structures, the granoblastic and gneiss-like structures typical for crystalline schists form another prevalent category of xenolith matter (Fig. 9), which implies that these granulites were formed in process of ferrogabbroid and ferroclinopyroxenite metamorphism. Eclogite-like rocks match eclogites in terms of their modal composition, but have low (4–7%) jadeite contents in clinopyroxene in garnet $Alm_{32–42}Grs_{15–19}Py_{43–48}$. At the same time, clinopyroxene itself includes 5.14 to 8.69 wt.% of Al_2O_3 in the absence of chrome. Also present are picroilmenite (3–8 vol.%, indicated below as %) and insignificant amounts of plagioclase (<5%) (Sharkov et al., 1992).

Garnet granulites have $An_{25–27}$ plagioclase contents of 5 to 80 vol.%, the average being 40–50%; it includes impurities, such as P_2O_5 (0.11 wt.%) and BaO (0.36 wt.%). Among other minerals, it is worth mentioning comparable amounts of the garnet being close in composition to the one observed in eclogite-like rocks, and aluminiferous clinopyroxene (4.04 to 5.63 wt.% of Al_2O_3). Brown titaniferous hornblende of the pargasite-kaersutite series (up to 5%) is less common and red-brown biotite (up to 3%) is even more rare. Gray aluminiferous spinel and individual apatite grains are present in some cases in addition to garnet. Ore mineral (picroilmenite) contents are 2 to 7 vol.%, and therefore the rocks are generally similar to metamorphosed analogs of ferrogabbroids formed as a result of crystallization of moderately-alkaline Fe–Ti basalts in deep-seated magmatic chambers in process of underplating (Mittlefehld, 1986; Esperanca and Garfunkel, 1986). Fe–Ti basalts of the Neoproterozoic rifting area, whose fragment is described in the northeast of Egypt (Stern et al., 1991), and which could then spread to the territory of the modern Arabia, are considered as possible effusive analog of these rocks.

Compositions of clinopyroxenes and garnets are described in the respective diagrams in Fig. 10 (microprobe studies of minerals of these and other lower crustal rocks studied are presented in (Sharkov et al., 1992)).

Secondary changes in this series of rocks are relatively small and typically represented by local plagioclase saussuritization and replacement of pyroxene with fibrous amphibole, as well as by development of significantly chloritic kelyphitic rims around garnet. Potassium feldspar veins and/or thin lenses of barium zeolite (harmotome) are observed in some cases as well.

The second group of deep-seated xenoliths is sharply different from the previous one. It is formed by *garnet megacrysts and coarse-grained garnet-clinopyroxene splices*. Megacrysts of garnet $Alm_{19–26}Grs_{12–13.5}Py_{59–67.5}$ are represented by large (up to 10 cm in diameter) rounded nodules, often with melted surface (Fig. 11). Garnet is typically

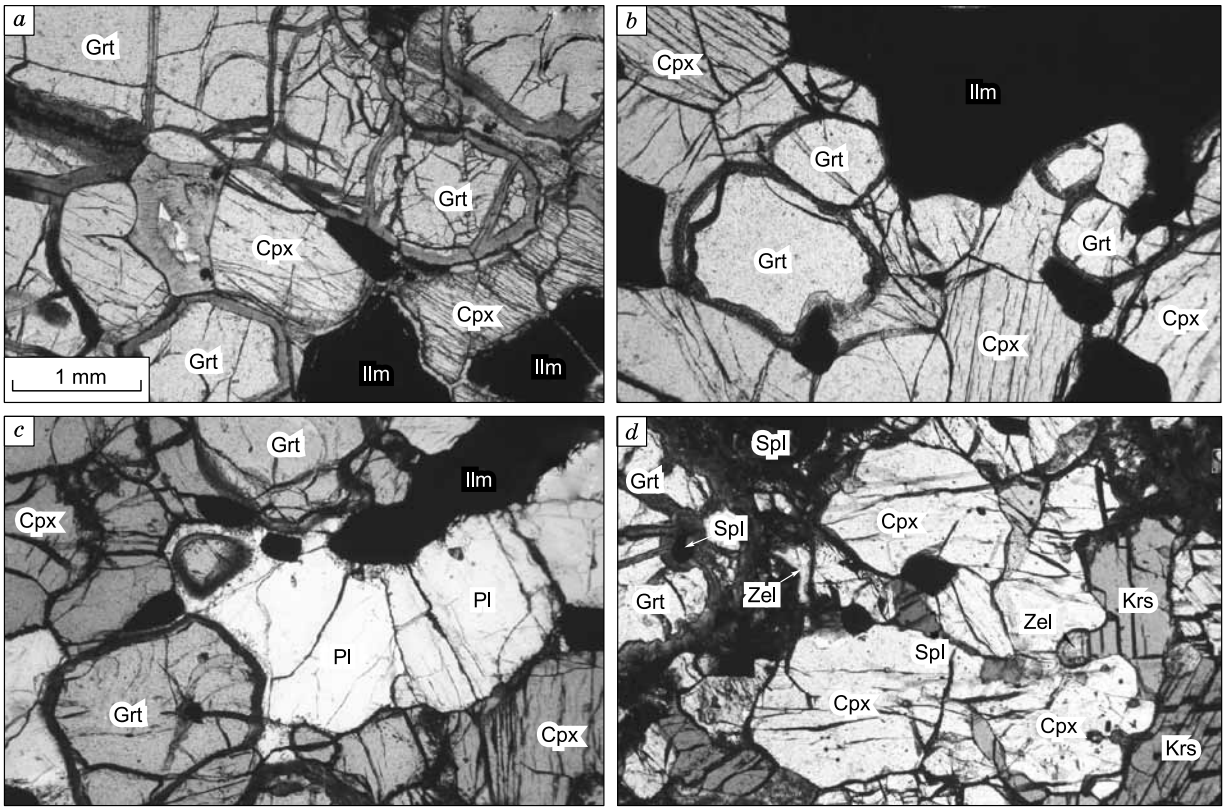

Fig. 9. Microfotoes of thin sections of xenoliths from the Nabi Matta diatreme, E.V. Sharkov's collection. *a*, *b*, Eclogite-like rocks (samples138-8 and 162-2); *c*, garnet granulite (sample 125-6); *d*, garnet-spinel-clinopyroxene-hornblende rock with Ba-zeolite (harmotome) (sample 125-3). Grt, garnet; Cpx, clinopyroxene; Krs, kaersutite; Pl, plagioclase; Ilm, ilmenite; Spl, spinel; Zel, harmotome (barium zeolite).

strongly fractured and two types of kelyphite often develop along the subparallel fracture system: in addition to significantly chloritic kelyphite similar to the one encountered in eclogite-granulite rocks, veins of fine-grained gabbro-norites with gray spinel are observed, which fill fractures with thicknesses of 0.1–0.3 mm (Sharkov et al., 1992). It seems that these kelyphites developed in different times, i.e., the chloritic ones occurred in lower crustal setting, where garnet megacrysts co-existed with garnet-granulites, and gabbro-norite veins appeared earlier and under different conditions. Similar veinlets in garnets of eclogite xenoliths in kimberlites are considered to be the result of garnet melting in course of decompression (Laz'ko et al., 1982), which seemingly took place in the considered case as well. Veinlets of the both types of kelyphites were subjected to melting at the surface of the garnet nodule as it was rising in the lamprophyre. Megacrysts of similar composition, which include gabbro-norite-type kelyphite, are described along with mantle peridotites in Miocene basalts of Jordan, where formation of these kelyphites is associated with garnet melting in process of decompression (Yassen, 2014).

In addition, we observed several splices of garnet with similar composition with large pale-green high-Al augite (fassaite) crystals (with lengths up to 3–5 cm) with deformation marks; Al_2O_3 content in it varied from 8.72 to 9.24 wt.%, Ti and Na contents being low (Sharkov et al., 1992)). It is possible that coarse-grained (up to pegmatoid size) garnet-pyroxene rocks probably associated with crystallization of island arc magmas at large depths were the source rocks for these splices and garnet megacrysts.

Coarse-grained splices of *garnet-clinopyroxene-hornblende rocks with spinel* and *megacrysts* and *splices of* Al–Ti-*augite and kaersutite* are the second common group of xenoliths (Sharkov et al., 1992). Not all samples of these rocks include garnet $Alm_{31}Grs_{17}Py_{52}$, and its content does not exceed 5%. It is usually associated with dark opaque spinel whose contents also reach 5% (Fig. 9). Clinopyroxene (Al–Ti-augite) and kaersutite are present in comparable quantities; barium zeolite (harmotome) is often observed in interstitial spaces between grains.

In general, this group is close to "black" series xenoliths in intraplate moderately-alkaline Fe–Ti basalts, including the ones described above, even though garnet is rarely found in them (Ionov, 1988; Sharkov and Bogatikov, 2015b). Here, kaersutite often includes gas cavities, similarly to the hornblende of the "black" series, which indicates that strongly fluidized melt/fluid was involved in its formation. As opposed to eclogite-granulite formations, these rocks were practically unaffected by superimposed processes.

Thus, products of Neoproterozoic underplating of intraplate Fe–Ti basalts and seemingly island arc magmas (garnet megacrysts and garnet-clinopyroxene splices, as well as

spinel gabbro-norites from other diatremes) are observed among lower crustal xenoliths of the Nabi Matta diatreme.

Geothermal barometry of rocks

According to the mineralogical geothermobarometry data (Mercier's Gr–Cpx geobarometer (Mercier, 1980) and Powell's geothermometer (Powell, 1985)), eclogite-granulite rocks were formed under pressures of 13.5–15.4 kbar (at depths of 45–54 km) and at temperatures of 965 to 1115 °C (Sharkov et al., 1992). It was already mentioned that in terms of origin these rocks are associated with the Neoproterozoic underplating of Fe–Ti-basaltic melts, which is evidenced by locally preserved gabbro structures. Solidified but still hot rocks were engaged in plastic deformations and recrystallization with generation of blastic structures peculiar for garnet granulites and eclogite-like rocks. These rocks are typical for continental lower crust, which in this case stretched to depths of at least 50–54 km.

In contrast to these rocks, the xenoliths formed by garnet megacrysts and coarse-grained garnet-clinopyroxene splices were subjected to the same pressures, i.e., they also were lower crustal, but at different temperatures, specifically 1300–1390 °C (Sharkov et al., 1992). Based on mineral composition, the origin of this group, as mentioned above, was most likely associated with crystallization of island arc magmas at large depths.

Clinopyroxene-hornblende rocks with garnet and spinel (analogous to "black" series mantle xenoliths in basalts) were formed under the *PT* parameters similar to those for garnet granulites, i.e., P = 12.6 kbar and T = 1100 °C. The absence of deformations and secondary changes in these rocks implied that the melts intruded in the stabilized lower crust, and this process was associated with lamprophyre diatreme formation.

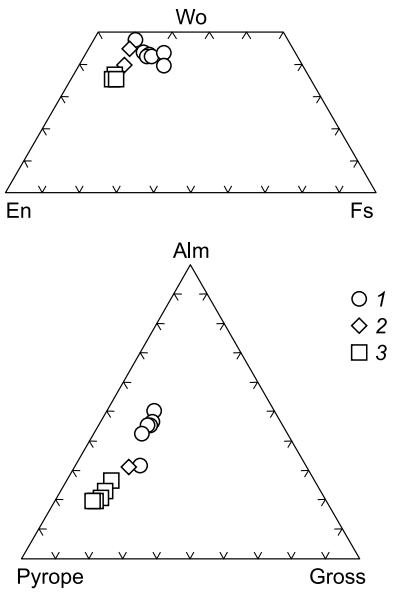

Fig. 10. Clinopyroxene and garnet compositions from main types of deep-seated xenoliths of the Nabi Matta diatreme. *1*, eclogite-granulite series; *2*, garnet-clinopyroxene-hornblende series; *3*, garnet-clinopyroxene splices.

Thus, the investigation of deep-seated xenolith populations in Cretaceous lamprophyre diatremes shows that the lower crust in the studied area was then primarily formed by the garnet granulites and eclogite-like rocks developed in the process of underplating of intraplate magmas. It is worth noting that these levels are presently occupied by mantle peridotites (see above), i.e., the initial crust is practically absent.

Fig. 11. Fractured garnet nodule with melting marks at the surface. Sample 138-9, E.V. Sharkov's collection.

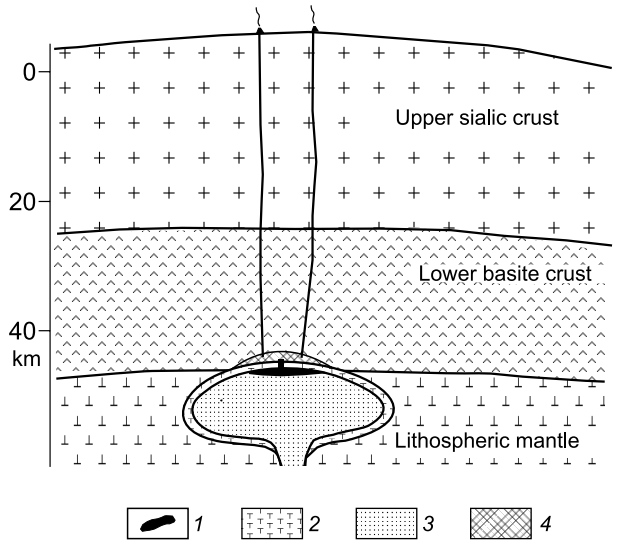

Fig. 12. Illustration of the lamprophyre diatreme formation. *1*, adiabatic melting zone of the minor plume head; *2*, cooled margin of the plume head; *3*, plume matter; *4*, zone of fluid component accumulation.

At the same time, the lower crustal mafite xenoliths dated with zircon isotope chronology (U–Pb) at ~560 Ma are found in xenolith populations in the Cenozoic basalts of Jordan along with the spinel peridotites typical for the mantle (Stern et al., 2016). Similarly to the studied rocks, these xenoliths often have granulite structures, but their composition and presence of relicts of cumulative structures match the norites and gabbro-norites formed, according to the cited authors, under back-arc sea conditions. Garnet was nearly absent from these xenoliths, and the researchers were unable to correctly identify the *PT* parameters of their formation apart from the temperature (702 to 891 °C). These discoveries may indicate that relicts of the ancient lower crust, especially those formed by relatively weakly metamorphosed rock types, may be preserved in the roofs of mantle plumes.

Lamprophyre diatreme formation

Lamprophyre diatremes of the Jebel Ansariya Ridge were formed 100 Ma earlier than the late Cenozoic mantle plume; they appear to be the manifestations of intraplate (plume) activity, although on a significantly smaller scale. The presence of basaltic bombs among the pyroclastic matter and small basaltic flows at the bottoms of many diatremes indicates that adiabatic melting of the plume matter took place here as well. Thus, we may conclude that local Cretaceous plume heads were small in size, and, according to the geobarometric data, spread deeper, than late Cenozoic ones. The presence of xenoliths analogous to those of the "black" series from basalts indicates that incongruent melting in cooled margins of these plume heads could take place as well (Sharkov and Bogatikov, 2015a).

The absence of Cretaceous diatremes of mantle peridotites in xenolith populations may imply that lamprophyres were most likely formed as a result of accumulation of the volatile components generated in process of decompression degassing of the mantle plume matter between its head and the roof; the newly formed basaltic melt spread to the same area as well (Fig. 12). When the roof of this reservoir was breached, an explosive outburst of the mixture of volatile components and basaltic melt (i.e., lamprophyre) occurred accompanied by trapping of lithospheric roof fragments.

DISCUSSION

It follows from the data presented that a thick mafic continental lower crust formed in the process of the Pan-African orogeny existed in the lithosphere of the northwestern Arabian plate as early as the Middle Cretaceous, and that its fragments are included in Cretaceous lamprophyre diatremes. However, the late Cenozoic basalts in the region barely show any traces of this crust in the xenoliths, while it is xenoliths of mantle peridotites that are now transported from these levels. The region was at its platform evolution stage between these events, and therefore the disappearance of the ancient lower crust here may only be associated with ascending of the late Cenozoic mantle plume, which led to strong basaltic magmatism. It was shown earlier that mantle plume heads could reach the basement of the upper (sialic) crust, while the lower crust matter was displaced by the spreading mantle plume matter (Fig. 6). The fact that the ancient upper (sialic) crust is preserved almost entirely in its original form implies that it was not involved in these processes.

Ascending of large amounts of mantle plume matter to the upper shells of the Earth should have initiated descending flows of cooled dense lower crustal matter. It is possible that in case of appearance of the late Cenozoic mantle plume beneath the western Arabian plate, Eastern Mediterranean in the west and South Caspian Basin in the east became the areas of descending mantle flows. According to the geophysical data, large negative isostatic anomalies are observed in these areas, which indicate the mass deficit, i.e., the present-day submergence of these structures (Sharkov et al., 2015).

It appears that the destruction of the ancient lower crust in the region is accompanied by the formation of new lower crust via underplating, i.e., accumulation of basaltic melt between the mantle plume head and the overlying ancient sialic crust (Fig. 6*b*). Thus, we might expect that the standard two-part structure of the continental crust in the region will eventually be restored.

It was shown earlier that margin only the fragments of the upper cooled margins of mantle plume heads occurred as mantle xenoliths in basalts above the adiabatic melting zone. Moreover, these xenoliths are only observed in the earliest fluid-saturated Fe–Ti alkaline-basaltic melts and they are absent in the evolved tholeiitic basalts. Thus, we infer that

plume protolith is rapidly depleted by fluids, especially alkalis, and that this source may produce melts on the other side of the critical undersaturation surface in the basaltic tetrahedron (Yoder and Tilley, 1962), i.e., tholeiitic basalts, that form the majority of LIPs, under the same *PT* parameters (Sharkov and Bogatikov, 2015a; Sharkov et al., 2017). It seems that the main growth of a new lower mafite crust is occurring at this particular stage from below via underplating process. Thus, the only thing that could be said about the newly formed lower crust below the trap areas, for example, the Siberian Permian-Triassic one, is that it was most likely being formed in that particular period.

Based on the data available, the same fluids that are included in the mantle plume matter, which ensures the formation of LIPs (see above), especially highly mobile carbonatite fluids/melts, are a significant component of lamprophyres and kimberlites. Their origin is most likely associated with the processes at the boundary outer (liquid) core and the mantle of the Earth. However, the explosive phenomena leading to capture of deep-seated xenoliths in the kimberlite-lamprophyre-basalt series occur at various depths and due to different causes: (1) in basalts—due to local accumulation of volcanic gases under the upper cooled margin of the plume head at the boundary with the adiabatic melting zone at depths of 20–24 km; and (2) in lamprophyres—also due to local accumulation of gas phases between a minor mantle plume head and the lower crust at depths of about 50–55 km. Xenolith trapping by lavas becomes a subordinate process in this cases. In kimberlites, however, the situation is reversed. According to the experimental data, as the CO_2-rich kimberlite melt rises, CO_2 solubility decreases rapidly at large depths (~200 km), which is accompanied by explosive CO_2 discharge. It leads to disintegration of lithospheric (both mantle and crust) rocks adjacent to the rapidly rising kimberlite melt and facilitates trapping and fast transporting of their fragments (xenoliths and xenocrystals, including diamonds) to the surface (Girnis and Ryabchikov, 2005).

CONCLUSIONS

1. Middle Cretaceous lamprophyre diatremes of the Jebal Ansaria Ridge include xenoliths of the ancient (Neoproterozoic) lower crust predominantly formed by garnet granulites and eclogite-like rocks generated by Fe–Ti-oxide gabbro and clinopyroxenites. Garnet megacrysts and splices of garnet with high-Al clinopyroxene, most likely formed by the activity of island arc magmas, are found among the xenoliths. Garnet-clinopyroxene-hornblende rocks close in their composition to mantle xenoliths of the "black" series in basalts seem to be the youngest rocks possibly associated with lamprophyre activity episodes; they may be fragments of the small intrusions adjacent to the diatremes. Xenoliths of mantle peridotites are absent in the studied populations.

2. On the contrary, late Cenozoic plateau basalts in the region barely include any lower crustal xenoliths (i.e., they are rare), whereas xenoliths of mantle spinel peridotites (mainly lherzolites) are well developed in the alkaline basalts; these peridotites contain veins of "black" series rocks (clinopyroxenites, clinopyroxene-hornblende rocks, hornblendites, phlogopitites, etc.), formed due to high-density fluid/melt activity. Both types of mantle xenoliths are most likely the fragments of the upper cooled margin of the plume head above the adiabatic melting zone transported to the surface by the newly formed basaltic melts.

3. Mantle xenoliths in basalts seem to represent two main types of the matter in thermochemical plume compositions: (1) mantle peridotites and (2) fluid components, which very probably arrived from the liquid core and initiated mantle plume ascent. In other words, the thermochemical mantle plume head matter is formed by depleted peridotites (mainly spinel lherzolites) and saturated with fluid components, which include Fe, Ti, alkalies, Ba, Nb, Ta, light rare earth elements, and other incompatible elements, as well as H_2O and CO_2.

4. According to the thermal barometric data, the "black" series rocks were formed at 826–980 °C at depths of 21–27 km (0.7–0.9 Ga); thus, plume heads could reach the depth of 21 km, i.e., the basement of the upper (sialic) crust. Green peridotites of the matrix were transported from the depths of 24–42 km (0.8–1.4 GPa). In the Middle Cretaceous, this depth interval was occupied by the lower continental crust displaced by late Cenozoic thermochemical mantle plume head spreading. The plume matter should have been less dense than peridotites and eclogites of the lithospheric mantle, but significantly denser then the upper (sialic) crust, which apparently determined the upper limit of the mantle plume head uplift.

5. Rare joint finds of lower crustal and mantle xenoliths in young basalts of the province indicate that remnants of the ancient lower crust could be locally preserved in the roofs of plume heads.

6. Based on the evidence available, we may conclude that the deep structure of the region changed radically in the late Cenozoic due to ascending of a mantle plume, the ancient upper sialic crust being the only remaining part of the original structure. The new lower crust will most likely be formed in time via underplating, thereby restoring the standard two-part structure of the continental crust section.

The authors thank RAS academician N.L. Dobretsov and the anonymous reviewer for valuable contributions to the manuscript.

The study was supported by the Program of the Presidium of the Russian Academy of Sciences No. 19 "Fundamental problems of geological and geophysical research of lithospheric processes" (project I.19 "Magmatism and fluid and mineral formation in the Earth's history").

REFERENCES

Artyushkov E.V., 1995. Physical Geodynamics [in Russian]. Nauka, Moscow.

Bogatikov, O.A., Kovalenko, V.I., Sharkov, E.V., 2010. Magmatism, Tectonics, and Geodynamics of the Earth. Relationships in Time and Space [in Russian]. Nauka, Moscow.

Brandon, A.D., Norman, M.D., Walker, R.J., Morgan, J.W., 1999. ^{186}Os–^{187}Os systematics of Hawaiian picrites. Earth Planet. Sci. Lett. 174 (1–2), 25–42.

Brey, G.P., Köhler, T., 1990. Geothermobarometry in four-phase lherzolites II. New thermobarometers, and practical assessment of existing thermobarometers. J. Petrol. 31 (6), 1353–1378.

Dawson, J.B., 1980. Kimberlites and Their Xenoliths [in Russian]. Springer-Verlag, Berlin–Heidelberg.

Dobretsov, N.L., 2008. Geological implications of the thermochemical plume model. Russian Geology and Geophysics (Geologiya i Geofizika) 49 (7), 441–454 (587–604).

Dobretsov, N.L., Kirdyashkin, A.G., Kirdyashkin, A.A., 2001. Deep-Level Geodynamics [in Russian]. Akad. Izd. Geo, Novosibirsk.

Dobretsov, N.L., Kirdyashkin, A.A., Kirdyashkin, A.G., 2006. Diameter and formation time of plume head at the base of refractory lithospheric layer. Dokl. Earth Sci. 406 (1), 55–60.

Downes, H., 2001. Formation and modification of the shallow sub-continental lithospheric mantle: a review of geochemical evidence from ultramafic xenolith suites and tectonically emplaced ultramafic massifs of Western and Central Europe. J. Petrol. 42 (1), 233–250.

Ernst, R.E., 2014. Large Igneous Provinces. Cambridge Univ. Press, Cambridge.

Esperanca, S., Garfunkel, Z., 1986. Ultramafic xenoliths from the Mt. Carmel area (Karem Maharal Volcano), Israel. Lithos 19 (1), 43–49.

Faccenna, C., Thorsten, W. Becker, T.W., Jolivet, L., Keskin, M., 2013. Mantle convection in the Middle East: Reconciling Afar upwelling, Arabia indentation and Aegean trench rollback. Earth Planet. Sci. Lett. 375, 254–269.

French, S.W., Romanowicz, B., 2015. Broad plumes rooted at the base of the Earth's mantle beneath major hotspots. Nature 525, 95–99.

Girnis, A.V., Ryabchikov, I.D., 2005. Generation of kimberlite magmas: Conditions and mechanisms. Geologiya Rudnykh Mestorozhdenii 47 (6), 524–536.

Grachev, A.F., Komarov, A.N., 1994. The new data on the uranium content in the continental and oceanic mantle. Fizika Zemli, No. 1, 3–9.

Hansen, S.E., Nyblade, A.A., Benoit, M.H., 2012. Mantle structure beneath Africa and Arabia from adaptively parameterized P-wave tomography: implications for the origin of Cenozoic Afro-Arabian tectonism. Earth Planet. Sci. Lett. 319–320, 23–34.

Ionov, D.A., 1988. Deep-seated ultramafic inclusions in basalts, in: Laz'ko, E.E., Sharkov, E.V. (Eds.), Magmatic Rocks, Vol. 5: Ultramafic Rocks [in Russian]. Nauka, Moscow, pp. 310–338.

Irving, A.J., 1980. Petrology and geochemistry of composite ultramafic xenoliths in alkalic basalts and implications for magmatic processes within the mantle. Am. J. Sci. 280-A, 2, 389–426.

Kaminsky, F.V., 2017. The Earth's Lower Mantle. Composition and Structure. Springer. DOI: 10.1007/978-3-319-55684-0.

Kirdyashkin, A.A., Kirdyashkin, A.G., 2016. On thermochemical mantle plumes with an intermediate thermal power that erupt on the Earth's surface. Geotectonics 50 (2), 209–222.

Kovalenko, V.I., Solovova, I.P., Naumov, V.B., Ryabchikov, I.D., Ionov, D.A., Tsepin, A.I., 1986. Mantle mineral formation with participation of a CO_2-sulfide-silicate fluid. Geochem. Int. 23 (7), 66–79.

Laz'ko, E.E., 1988. Deep-seated ultramafic inclusions in kimberlites, in: Laz'ko, E.E., Sharkov, E.V. (Eds.), Magmatic Rocks, Vol. 5: Ultramafic Rocks [in Russian]. Nauka, Moscow, pp. 346–379.

Laz'ko, E.E., Serenko, V.P., Koptil', V.I., Rudnitskaya, V.I., Zepin, A.I., 1982. Kyanite diamondiferous eclogites from the kimberlite pipe Sytykanskaya (Yakutia). Izvestiya AN SSSR, Ser. Geol., No. 7, 35–46.

Ma, G.S.-K., Wang, K.-L., Malpas, J., Iizuka, Y., Xenophontos, C., Turkmani, A.A., Chan, G.H.-N., Usuki, T., Chan, Q.H.-S., 2015. Melt-pockets and spongy clinopyroxenes in mantle xenoliths from the Plio-Quaternary Al Ghab volcanic field, NW Syria: implications for the metasomatic evolution of the lithosphere, in: Khan, A., Deschamps, F. (Eds.), The Earth's Heterogeneous Mantle. Springer Int. Publ., Cham, pp. 205–257.

Maruyama, S., 1994. Plume tectonics. J. Geol. Soc. Japan 100, 24–49.

Mercier, J.C., 1980. Single-pyroxene thermobarometry. Tectonophysics 70, 1–37.

Mittlefehld, D.W., 1986. Petrology of high pressure clinopyroxenite series xenoliths. Mount Carmel. Israel. Contrib. Miner. Petrol. 94 (2), 245–252.

Pearson, D.G., Canil, D., Shirey, S.B., 2003. Mantle samples included in volcanic rocks: xenoliths and diamonds, in: Treatise on Geochemistry, Vol. 2. Elsevier, Amsterdam, pp. 172–221.

Ponikarov, V.P., Kaz'min, V.G., Kozlov, V.V., Krasheninnikov, V.A., Mikhailov, I.A., Razvalyaev, A.V., Sulidi-Kondrat'ev, E.D., Uflyand, A.K., Faradzhev, V.A., Geology and Mineral Resources of Foreign Countries. Syria [in Russian]. Nedra, Leningrad.

Powell, R., 1985. Regression diagnostics and robust regression in geothermometer/geobarometer calibration: the garnet-clinopyroxene geothermometer revisited. J. Metamorph. Geol. 3 (3), 231–243.

Puchtel, I.S., Brugmann, G.E., Hofmann, A.W., 1999. Precise Re–Os mineral isochron and Pb–Nd–Os isotope systematics of a mafic-ultramafic sill in the 2.0 Ga Onega plateau (Baltic Shield). Earth Planet. Sci. Lett. 170, 447–461.

Putirka, K., 2008. Thermometers and barometers for volcanic systems, in: Putirka, K., Tepley, F. (Eds.), Minerals, Inclusions and Volcanic Processes, Rev. Min. Geochem. 69. Mineral. Soc. Am. pp. 61–120.

Rudnick, R.L., 1960. Growing from below. Nature 347 (6295), 711–712.

Ryabchikov, I.D., Sharkov, E.V., Kogarko, L.N., 2010. Rhönite from mantle peridotites in Syria. Bull. Tethys Geol. Soc., Cairo, pp. 9–13.

Schaeffer, A.J., Lebedev, S., 2013. Global shear speed structure of the upper mantle and transition zone. Geophys. J. Int. 194, 417–449. DOI: 10.1093/gji/ggt095.

Sharkov, E.V., Bogatikov, O.A., 2010. Tectonomagmatic evolution of the Earth and Moon. Geotectonics 44 (2), 85–101.

Sharkov, E.V., Bogatikov, O.A., 2015a. "Roots" of magmatic systems in the large continental igneous provinces. Dokl. Earth Sci. 460 (2), 154–158.

Sharkov, E.V., Bogatikov, O.A., 2015b. The problem of evolution of the Earth's core: Geological, petrological, and paleomagnetic evidence. Dokl. Earth Sci. 462 (1), 533–538.

Sharkov, E.V., Bogatikov, O.A., 2015c. Processes accompanying emplacement of a mantle plume in the continental lithosphere: The example of West Syria. Dokl. Earth Sci. 463 (2), 802–807.

Sharkov, E.V., Jermakani, E., Hanna, S., Bagdasaryan, G.P., 1988. First K–Ar dates for kimberlitic rock diatremes in the coastal part of Syria. Dokl. AN SSSR 301 (4), 943–946.

Sharkov, E.V., Laz'ko, E.E., Hanna, S., 1992. Deep-seated inclusions in the Nabi-Matta explosive center (northwest Syria). Geokhimiya, No. 9, 1241–1261.

Sharkov, E.V., Snyder, G.A., Taylor, L.A., Laz'ko, E.E., Jerde, E., Hanna, S., 1996. Geochemical peculiarities of the asthenosphere beneath the Arabian plate: Evidence from mantle xenoliths of the quaternary Tell-Danun Volcano (Syrian-Jordan Plateau, Southern Syria). Geochem. Int. 34 (9), 737–752.

Sharkov, E., Lebedev, V., Chugaev, A., Zabarinskaya, L., Rodnikov, A., Sergeeva, N., Safonova, I., 2015. The Caucasian–Arabian segment of the Alpine–Himalayan collisional belt: Geology, volcanism and neotectonics. Geosci. Front. 6 (4), 513–522.

Sharkov, E., Bogina, M., Chistyakov, A., 2017. Magmatic systems of large continental igneous provinces. Geosci. Front. 8 (4), 621–640.

Sobolev, N.V., 1977. Deep-Seated Inclusions in Kimberlites and the Problem of the Composition of the Upper Mantle. Am. Geophys. Union, Washington, DC.

Sobolev, N.V., Abu-Assale, H., Kepezhinskas, V.V., Kepezhinskas, K.B., Sharaf, M., Fallahah, A., Kireev, A.D., 1990. Lampro-

phyres of Cretaceous diatremes on the Syrian rift. Dokl. AN SSSR 314 (2), 435–438.

Stern, R.J., Kröner, A., Rashwan, A.A., 1991. A late Precambrian (~710 Ma) high volcanicity rift in the southern Eastern Desert of Egypt. Geologische Rundschau 80 (1), 155–170.

Stern, R.J., Ali, K., Ren, M., Jarrar, G.H., Romer, R.L., Leybourne, M., Whitehouse, M.J., 2016. Cadomian (~560 Ma) crust buried beneath the Northern Arabian Peninsula: mineral, chemical, geochronological, and isotopic constraints from NE Jordan xenoliths. Earth Planet. Sci. 436, 31–42.

Taylor, W.R., 1998. An experimental test of some geothermometer and geobarometer formulations for upper mantle peridotites with application to the thermobarometry of fertile lherzolite and garnet websterite. Neues Jahrbuch für Mineralogie-Abhandlungen 172, 381–408.

Walker, R.J., Morgan, J.W., Hanski, E.J., Smolkin, V.F., 1997. Re–Os systematics of early Proterozoic ferropicrites, Pechenga complex, northwestern Russia: evidence for ancient ^{187}Os-enriched plume. Geochim. Cosmochim. Acta 61, 3145–3160.

Wilshire, H.G., Pike, J.E.N., Meyer, C.E., Schwarzman, E.C., 1980. Amphibole-rich veins in lherzolite xenoliths, Dish Hill and Deadman Lake, California. Am. J. Sci. 280-A, 576–593.

Witt-Eickschen, G., Seck, H.A., 1991. Solubility of Ca and Al in orthopyroxene from spinel peridotite: an improved version of an empirical geothermometer. Contrib. Mineral. Petrol. 106, 431–439.

Yarmolyuk, V.V., Kovalenko, V.I., 2003. Deep Geodynamics and Mantle Plumes: Their Role in the Formation of the Central Asian Fold Belt Petrology 11 (6), 504–531.

Yassen, I.A.A.B., 2014. Petrography and mineral chemistry of the almanden garnet, and implication for kelyphite texture in the Miocene alkaline basaltic rocks North Eastern Jourdan. Int. J. Geosci. 5, 222–237.

Yoder, H.S., Tilley, C.E., 1962. Origin of basalt magmas: An experimental study of natural and synthetic rock systems. J. Petrol. 3 (3), 342–532.

Zolotukhin, V.V., Vilenskii, A.M., Dyuzhikov, O.A., 1986. Basalts of the Siberian Platform [in Russian]. Nauka, Novosibirsk.

Editorial responsibility: N.L. Dobretsov